

Primary role of the structural phase transition in the strongly coupled structure and magnetism of $\text{La}_{0.835}\text{Sr}_{0.165}\text{MnO}_3$ single crystal

K. V. Kamenev

Department of Physics, University of Warwick, Coventry CV4 7AL, United Kingdom

G. J. McIntyre

Institut Laue-Langevin, 156X, 38042 Grenoble Cedex, France

D. McK Paul, M. R. Lees, and G. Balakrishnan

Department of Physics, University of Warwick, Coventry CV4 7AL, United Kingdom

(Received 21 January 1998)

We report a neutron diffraction investigation of the role of pressure on the strong coupling between the structural and ferromagnetic phase transitions in $\text{La}_{0.835}\text{Sr}_{0.165}\text{MnO}_3$. The results are summarized in the form of a pressure-temperature phase diagram and reveal the dominant character of the structural changes with respect to the magnetic transitions, which results in a broad metastable area around the crossing point of the structural and magnetic phase transitions. The phase diagram contains a number of extremely unusual features including the pressure independence of the Curie temperature in the orthorhombic phase, a reentrance of the rhombohedral phase at low temperatures, and a change of the type of the magnetic phase transition from second order to first order due to the strong coupling between the structural and the magnetic properties of this material. [S0163-1829(98)52212-6]

The $\text{La}_{1-x}\text{A}_x\text{MnO}_3$ (where A is Ca or Sr) series of compounds have proved to be extremely useful as model systems when investigating the physics found in this class of perovskite materials. Evidence for new electronic states¹ and magnetic polarons,² the observation of a giant oxygen isotope shift,³ reports of a current switching of resistive states,⁴ and magnetic-field-induced change in structure^{5,6} as well as colossal magnetoresistance (CMR) near the ferromagnetic spin ordering temperature T_C (Refs. 7 and 8) were all first reported from studies on these materials. In this paper we present experimental data on the magnetic and structural phase transitions in $\text{La}_{0.835}\text{Sr}_{0.165}\text{MnO}_3$ under pressure. The use of pressure as a thermodynamic variable provides us with a simple but powerful means by which to modify the interactions within the system without changing the doping level.

The parent compound of the $\text{La}_{1-x}\text{Sr}_x\text{MnO}_3$ series, LaMnO_3 , is an antiferromagnetic insulator below 140 K. Chemical substitution of the La^{3+} by Sr^{2+} brings about a ‘‘double-exchange’’ interaction between the Mn^{3+} and the Mn^{4+} ions,⁹ and for $x \approx 0.15$, induces a ferromagnetic metallic ground state.^{10,11} Close to the Curie temperature, T_C , the application of a magnetic field can produce up to a thousand fold decrease in resistivity.^{7,8} Doping with Sr also results in a change from an orthorhombic ($Pbnm$; $Z=4$) to a rhombohedral ($R\bar{3}c$; $Z=2$) structure. T_C increases with x , from 238 K for $x=0.15$ to 283 K for $x=0.175$. In contrast, the temperature of the structural transition, T_S , decreases from 380 to 190 K over the same doping range. For a critical doping level $x_c \approx 0.17$ the lines on the $x-T$ phase diagram marking the magnetic and structural phase transitions intersect at a temperature of 270 K.¹¹ Due to the sensitivity of T_C and T_S to the Sr concentration in the vicinity of the crossing point,

different research groups disagree about the estimated value of x_c . For example, in zero field and ambient pressure the sample used in Ref. 5 and reported to have $x=0.170$ exhibits the structural $R\bar{3}c \rightarrow Pbnm$ phase transition at 280 K and magnetic transition at 260 K which means that this sample is situated ‘‘on the left’’ of the crossing point on the $x-T$ phase diagram. For samples with $x \approx 0.165$ (i.e., $x < x_c$) the application of a magnetic field at temperatures immediately below T_S induces a structural phase transition back from the $Pbnm$ to the $R\bar{3}c$ state.^{5,6} Similar phenomena have been found on application of pressure.¹²⁻¹⁴ Recently it has been shown by strain-gauge dilatometry that for a sample with $x=0.165$ the temperatures of the structural and magnetic phase transitions can be brought together by application of hydrostatic pressure of approximately 3 kbar,¹³ i.e., under a pressure of approximately 3 kbar, $T_S = T_C$. In the present study we perform not only temperature but also pressure scans and use neutron diffraction to monitor directly the changes in the magnetic and structural phases of a single crystal of $\text{La}_{0.835}\text{Sr}_{0.165}\text{MnO}_3$.

The measurements have been carried out on single crystals of $\text{La}_{0.835}\text{Sr}_{0.165}\text{MnO}_3$ grown in an infrared image furnace using the floating-zone method. The details of sample preparation are described elsewhere.^{6,13} Neutron diffraction measurements were carried out using the single-crystal diffractometer $D10$ at the Institut Laue-Langevin in Grenoble, France. The orthorhombic (200) and (405) reflections were chosen to monitor the magnetic and structural phase transitions, respectively. A high-pressure cell using gaseous helium as a pressure-transmitting medium was used as the sample environment. This equipment allowed us to change temperature and pressure *in situ* and to conduct the measurements continuously at temperatures between 1.2 and 310 K and pressures of up to 5 kbar.

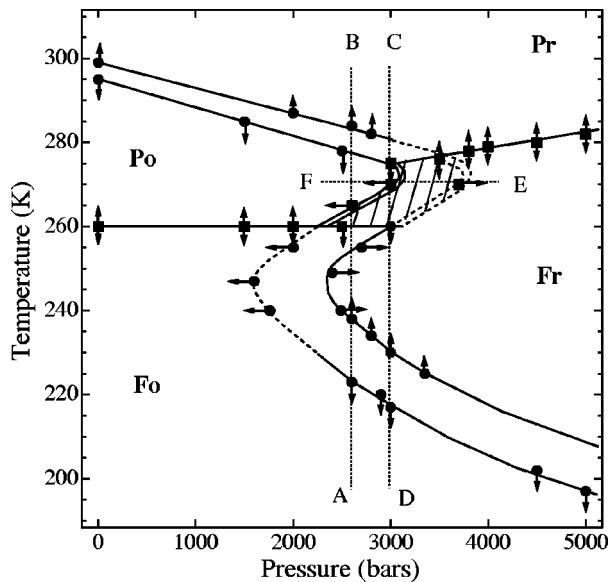


FIG. 1. The structural and magnetic P - T phase diagram of $\text{La}_{0.835}\text{Sr}_{0.165}\text{MnO}_3$. The phases are Pr, paramagnetic rhombohedral; Po, paramagnetic orthorhombic, Fo, ferromagnetic orthorhombic Fr, ferromagnetic rhombohedral. The Curie temperatures T_C and the temperatures of the structural phase transitions T_S are marked with square and circle symbols, respectively. The hatched area indicates the area of the crossing point. The arrows show the directions of the temperature or pressure scans at each measurement point.

Due to the complexity of the features presented on the P - T phase diagram, we feel it is necessary to present the diagram itself first and then to concentrate on its details. The “pressure-temperature” phase diagram of $\text{La}_{0.835}\text{Sr}_{0.165}\text{MnO}_3$ is created by the two boundaries of the structural and magnetic phase transitions (Fig. 1). The first-order structural phase transition is shown by the two “Z”-shaped curves enclosing the metastable region where, depending on the (P, T) history of the sample, either the rhombohedral or the orthorhombic phase can occur. The single line which starts at $T_C = 261$ K at ambient pressure and ends at 282 K under a pressure of 5 kbar corresponds to the second-order paramagnetic \rightarrow ferromagnetic phase transition. The arrows show the directions of the temperature or pressure scans at each measurement point. The hatched area indicates the region of intersection of T_S and T_C and separates four phases each with different combinations of structural ($R\bar{3}c$ or $Pbnm$) and magnetic (paramagnetic or ferromagnetic) order. These phases are marked on the diagram as Pr, Po, Fo, or Fr, where “P” or “F” specify the magnetic state as paramagnetic or ferromagnetic while “r” or “o” describe the structural symmetry as rhombohedral ($R\bar{3}c$) or orthorhombic ($Pbnm$), respectively. One of the key features of the phase diagram is that due to the peculiar Z shape of the phase boundaries near the crossing point, some of the lines of the phase transitions cannot be seen by temperature scans alone. The portions of the phase boundaries which can be observed during a temperature scan at a constant pressure are delineated by solid lines. The phase boundaries shown by broken lines represent the transitions which can only be detected by isothermal pressure changes.

Initially, we consider the phase transitions which occur during isobaric temperature scans. The temperature T_{S1} of the Pr \rightarrow Po transition (high-temperature low-pressure part of the phase diagram) decreases linearly with applied pressure ($dT_{S1}/dP = -6.1$ K/kbar) and disappears abruptly at $P = 3.0$ kbar. For less than 3 kbar, the second-order Po \rightarrow Fo magnetic phase transition seen at $T_C = 261$ K is pressure independent. Under a pressure of about 2.4 kbar we observe a re-entrance of the rhombohedral $R\bar{3}c$ phase at the temperature T_{S2} ($T_{S2} < T_{S1}$, $dT_{S2}/dP > 0$) but this time within a ferromagnetically ordered state (Fr). As the temperature is decreased still further, the sample undergoes a phase transition at T_{S3} (low-temperature high-pressure part of the phase diagram) to a ferromagnetic orthorhombic (Fo) phase. The phase transitions at T_{S1} and T_{S3} both lie on the same boundary of the phase transitions from the rhombohedral to the orthorhombic state. However, we need to vary the pressure at a fixed temperature in order to complete this line and join these two points on the phase diagram (see below). It is important to note that in the pressure region up to 2.4 kbar, the Po \rightarrow Fo phase transition is still of second-order. If the sample is cooled under a pressure between 2.4 and 3.0 kbar, for example along the path BA shown on the P - T phase diagram, to a temperature T where $261 \text{ K} > T > T_{S2}$, i.e., without entering the Fr phase, then on heating, the reverse magnetic phase transition Fo \rightarrow Po occurs at 261 K with no hysteresis. However, if the sample is cooled sufficiently to enter the Fr regime, i.e., below T_{S2} , then during a subsequent heating run, both the structural $R\bar{3}c \rightarrow Pbnm$ and the magnetic $F \rightarrow P$ phase transitions occur simultaneously as a Fr \rightarrow Po transition.

To illustrate this behavior we present the temperature dependence of the integrated intensities of (405) and (200) reflections measured during heating at a pressure of 2.6 kbar along the path AB on the P - T phase diagram [Fig. 2(a)]. The structural phase transitions can be monitored by noting the changes in the intensity of the (405) reflection which is only present in the orthorhombic phase. As the temperature increases the sample undergoes a series of structural phase transitions: $Pbnm \rightarrow R\bar{3}c$ at $T_{S3} = 238$ K, $R\bar{3}c \rightarrow Pbnm$ at $T_{S2} = 264$ K and $Pbnm \rightarrow R\bar{3}c$ at $T_{S1} = 284$ K. The intensity of the magnetic (200) peak goes to zero at $T_C = 264$ K indicating that the magnetic phase transition occurs at the same temperature as the second structural transition, i.e., $T_C = T_{S2}$. The hysteresis in temperature of the magnetic phase transition increases as pressure increases above 2.4 kbar. This brings us to a very important conclusion: in the hatched area the behavior of the magnetic sublattice reflects the structural changes, switching the type of the magnetic phase transition from second order to first order.

The temperature T_{S2} and locked to it T_C of the Fr \rightarrow Po phase transition increase with applied pressure from 2.4 kbar to just below 3.0 kbar. At a pressure of 3.0 kbar the Po \rightarrow Fo phase transition boundary meets the line marking the structural Fo \rightarrow Fr transition. The intensities of the (405) and (200) reflections measured on cooling at 3.0 kbar along the path CD on the P - T phase diagram are presented in Fig. 2(b). The structural Pr \rightarrow Po phase transition occurs at $T_{S1} = 275$ K. Below T_{S1} the intensity of the (200) peak increases slightly with decreasing temperature, which may be indica-

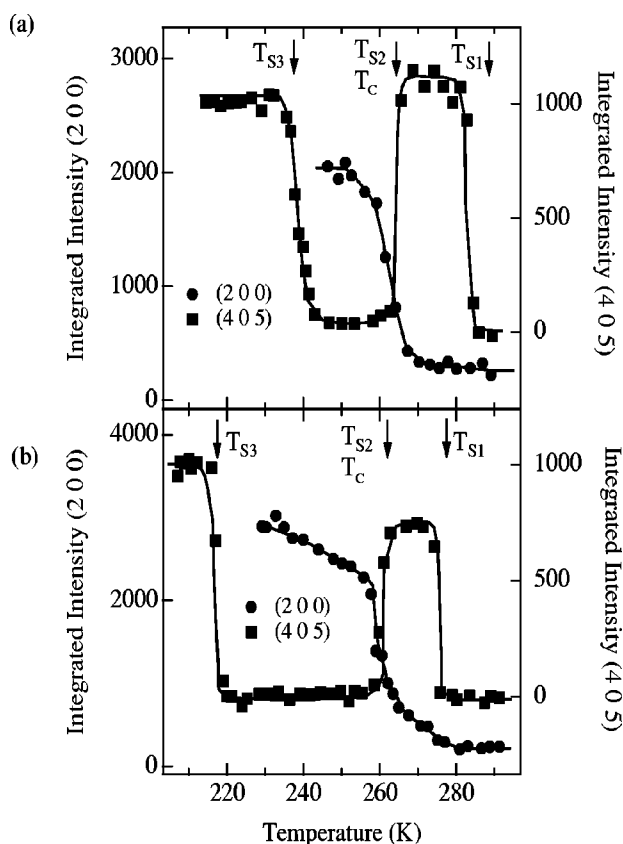


FIG. 2. Temperature dependencies of the intensities of (405) and (200) reflections measured on heating at 2.6 kbar along the path AB (a) and on cooling at 3.0 kbar along the path CD (b) on the P - T phase diagram. The low-temperature part of the (200) reflection is omitted for clarity.

tive of a degree of short range order, until at $T_{S2}=261$ K there is a rapid increase in slope reflecting a simultaneous structural and magnetic $Po \rightarrow Fr$ transition. Further cooling brings about a $Fr \rightarrow Fo$ phase transition at $T_{S3}=217$ K with the reappearance of the orthorhombic state.

The $Pr \rightarrow Po$ and $Fr \rightarrow Po$ phase boundaries on the P - T phase diagram intersect at a pressure of 3.0 kbar and temperature of about 275 K. On cooling under pressures higher than 3.0 kbar the magnetic $Pr \rightarrow Fr$ phase transition occurs at a higher temperature than the structural transition. As with the $Po \rightarrow Fo$ transition, which takes place in the orthorhombic $Pbnm$ phase under pressures lower than 3.0 kbar, the $Pr \rightarrow Fr$ phase transition is of second order. Nevertheless, in sharp contrast to the pressure-independent T_C seen in the orthorhombic phase below 3 kbars, the Curie temperature in the rhombohedral phase increases linearly with applied pressure with a $dT_C/dP=3.5$ K/kbar. Given that the cell volume is almost identical in the orthorhombic and the rhombohedral structures⁵ the change in the pressure dependence of T_C is especially intriguing. To understand this we note that the Curie temperature, as well as the magnitude of the CMR effect in this class of materials, is sensitive to the Mn-O-Mn bond angle.^{15,16} When the crystal is compressed in the $Pbnm$ phase, the Mn-O-Mn bonds are “in-plane” and the pressure does not affect them much, changing instead the interplane distances. In the rhombohedral phase the “easy” direction of compression is the threefold axis which forms a nonzero

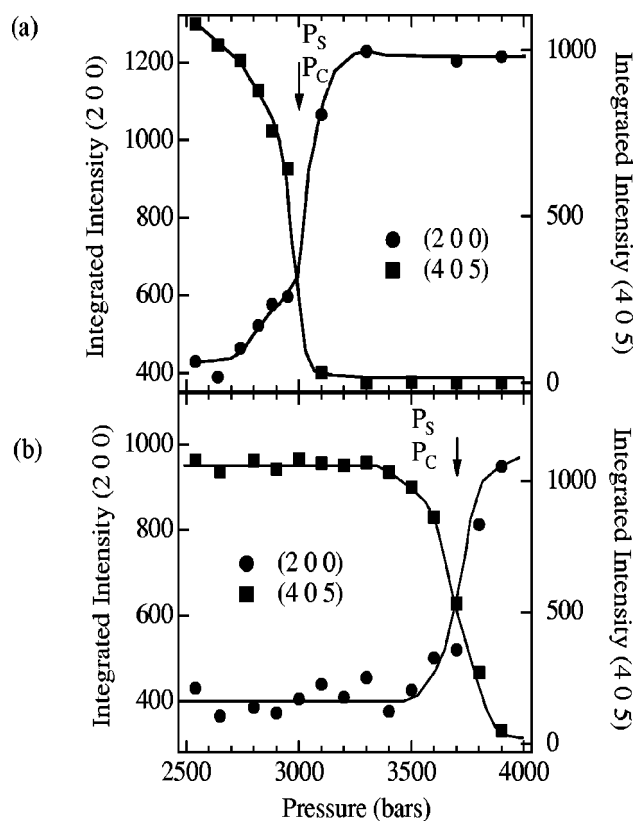


FIG. 3. Pressure dependencies of the intensities of (405) and (200) reflections measured at $T=270$ K on pressure release along path EF (a) and on pressure increase along path FE (b) on the P - T phase diagram.

angle to the Mn-O-Mn bonds. As a result, such bonds are affected more easily by applied pressure in the $R\bar{3}c$ structure. The temperature T_{S3} of the structural $Fr \rightarrow Fo$ transition decreases rapidly ($dT_{S3}/dP \approx -10.0$ K/kbar) in the pressure region above 3.0 kbar. The value of $dT_C/dP=3.5$ K/kbar given in the present paper was derived from the data obtained in the pressure region up to 5 kbar while in Ref. 13 the first experimental point after the crossing point was taken at 4 kbar and the pressure coefficient was estimated from three (P, T) points at $P=4, 5$ and 9 kbar. The pressure dependence of T_C is still steep just above the crossing point but it flattens as pressure increases above 4–5 kbar.

The results of the isobaric temperature scans have allowed us to establish some phase boundaries and to determine that the pressures 2.4 and 3.0 kbar are special for the phase diagram. It is evident that the high-temperature structural $Pr \rightarrow Po$ phase transition disappears abruptly at $P > 3.0$ kbar. The low-temperature series of $Po \rightarrow Fr \rightarrow Fo$ transitions appears above 2.4 kbar and exists only up to 3.0 kbar where the $Po \rightarrow Fr$ phase transition vanishes suddenly on crossing the magnetic $Po \rightarrow Fo$ phase transition at $T=261$ K and $P=3$ kbar. This effect is similar to the sharp drop of T_S in an applied magnetic field of about 2 T on the H - T phase diagram.⁵

The temperatures of the $Pr \rightarrow Po$ and $Fr \rightarrow Po$ phase transitions approach each other as the pressure nears 3.0 kbar, whilst the temperatures of the $Fo \rightarrow Fr$ and $Po \rightarrow Fr$ phase transitions coincide at 2.4 kbar. Although it is possible

to imagine that the lines of the structural phase transitions on the $P-T$ phase diagram have a change in slope at $P = 3.0$ kbar, $T \approx 273$ K, and $P = 2.4$ kbar, $T \approx 245$ K, it is not clear from the temperature scans what happens to the lines of the reverse Po \rightarrow Pr and Fr \rightarrow Fo phase transitions at pressures higher than 3.0 kbar and lower than 2.4 kbar, respectively. These boundaries as well as the line of the Po \rightarrow Fo magnetic phase transition must join together somewhere on the phase diagram. To connect the phase boundaries and to complete the phase diagram we have performed several isothermal pressure scans at temperatures above and below the horizontal line of the magnetic phase transition at 261 K. The changes in the intensities of the (405) and (200) reflections at $T = 270$ K during a decreasing pressure scan along the path EF and with increasing pressure along FE are presented in Figs. 3(a) and 3(b), respectively. The structural and magnetic phase transitions occur simultaneously at 3.0 kbar for decreasing and 3.7 kbar for increasing pressure. Isothermal pressure scans below 261 K have shown that the Fr \rightarrow Fo phase transition is induced by pressure release at pressures below 3.0 kbar.

Using the values for the temperatures and pressures of the phase transitions found during pressure scans we can connect the phase boundaries which were "invisible" for heating and cooling runs. Due to the hysteretic character of the first-order structural phase transition and the fact that the magnetic transition is tied to it, the crossing "point" occupies a hatched area on the $P-T$ phase diagram. In this area the sample can

adopt either a Fr or a Po state depending on the pressure-temperature path by which it was brought into the area. The isothermal pressure scans have helped us to establish that the lines on the $P-T$ phase diagram marking the structural phase transitions have a "Z" shape due to the re-entrant nature of the transition from the rhombohedral to orthorhombic phase. It is also clear from the phase diagram that the line of the magnetic phase transition mirrors the hysteresis loop of the structural phase transition within the hatched area. This reinforces our conclusion that in this region of the phase diagram it is the structural change which is driving the magnetic transition.

Finally, a comparison of the $x-T$,^{10,11} $H-T$,⁵ and $P-T$ phase diagrams reveals a common trend in the behavior of $\text{La}_{1-x}\text{Sr}_x\text{MnO}_3$ ($x \approx 0.165$), i.e., increase in Sr content, magnetic field and/or pressure leads to a crossing of T_S and T_C . We suggest that the abrupt decrease of T_S near $\mu_0 H = 2$ T (Ref. 5) is related to the intersection within the temperature-magnetic field plane of the line marking the magnetic phase transition and the boundary between the two phases with different structures. A comprehensive study of the hatched area of the phase diagram is possible, if temperature and one other parameter—either x , H , or P —can be varied. Since isothermal scans of Sr content (x) are clearly impossible and there are difficulties with the definition of T_C in magnetic field, the use of pressure as the second variable provides us with the only practical means of probing this complicated phase diagram.

¹J.-S. Zhou, W. Archibald, and J. B. Goodenough, *Nature* (London) **381**, 770 (1996).

²J. M. De Teresa *et al.*, *Nature* (London) **386**, 256 (1997).

³G. M. Zhao *et al.*, *Nature* (London) **381**, 676 (1996).

⁴A. Asamitsu *et al.*, *Nature* (London) **388**, 50 (1997).

⁵A. Asamitsu *et al.*, *Nature* (London) **373**, 407 (1995).

⁶A. J. Campbell *et al.*, *Phys. Rev. B* **55**, R8622 (1997).

⁷K. Chahara *et al.*, *Appl. Phys. Lett.* **63**, 1990 (1993).

⁸R. von Helmolt *et al.*, *Phys. Rev. Lett.* **71**, 2331 (1993).

⁹P.-G. de Gennes, *Phys. Rev.* **118**, 141 (1960).

¹⁰Y. Tokura *et al.*, *J. Phys. Soc. Jpn.* **63**, 3931 (1994).

¹¹H. Kawano *et al.*, *Phys. Rev. B* **53**, R14 709 (1996).

¹²M. Itoh *et al.*, *Phys. Rev. B* **55**, 14 408 (1997).

¹³K. Kamenev *et al.*, *Phys. Rev. B* **56**, 2285 (1997).

¹⁴Y. Moritomo, A. Asamitsu, and Y. Tokura, *Phys. Rev. B* **56**, 12 190 (1997).

¹⁵J. Fontcuberta *et al.*, *Phys. Rev. Lett.* **76**, 1122 (1996).

¹⁶J. F. Mitchell *et al.*, *Phys. Rev. B* **54**, 6172 (1996).